Determination of Grain Boundary Charging in $Cu(In,Ga)Se_2$ Thin Films

Preprint

C.-S. Jiang, M. A. Contreras, I. Repins,
H. R. Moutinho, R. Noufi, and M. M. Al-Jassim

Presented at the 2012 IEEE Photovoltaic Specialists Conference
Austin, Texas
June 3–8, 2012

Conference Paper
NREL/CP-5200-54111
June 2012

Contract No. DE-AC36-08GO28308

Available electronically at http://www.osti.gov/bridge

Available for a processing fee to U.S. Department of Energy
and its contractors, in paper, from:

U.S. Department of Energy
Office of Scientific and Technical Information

P.O. Box 62
Oak Ridge, TN 37831-0062
phone: 865.576.8401
fax: 865.576.5728
email: mailto:reports@adonis.osti.gov

Available for sale to the public, in paper, from:

U.S. Department of Commerce
National Technical Information Service
5285 Port Royal Road
Springfield, VA 22161
phone: 800.553.6847
fax: 703.605.6900
email: orders@ntis.fedworld.gov
online ordering: http://www.ntis.gov/help/ordermethods.aspx

Cover Photos: (left to right) PIX 16416, PIX 17423, PIX 16560, PIX 17613, PIX 17436, PIX 17721

Printed on paper containing at least 50% wastepaper, including 10% post consumer waste.

Determination of Grain Boundary Charging in $Cu(In,Ga)Se_2$ Thin Films

C.-S. Jiang, M.A. Contreras, I. Repins, H.R. Moutinho, R. Noufi, and M.M. Al-Jassim

National Renewable Energy Laboratory, Golden, CO 80401 USA

Abstract — **Surface potential mapping of $Cu(In,Ga)Se_2$ (CIGS) thin films using scanning Kelvin probe force microscopy (SKPFM) aims to understand the minority-carrier recombination at the grain boundaries (GBs) of this polycrystalline material by examining GB charging, which has resulted in a number of publications. However, the reported results are highly inconsistent. In this paper, we report on the potential mapping by measuring wide-bandgap or high-Ga-content films and by using a complementary atomic force microscopy-based electrical technique of scanning capacitance microscopy (SCM). The results demonstrate consistent, positively charged GBs on our high-quality films with minimal surface defects/charges. The potential image taken on a low-quality film with a 1.2-eV bandgap shows significantly degraded potential contrast on the GBs and degraded potential uniformity on grain surfaces, resulting from the surface defects/charges of the low-quality film. In contrast, the potential image on an improved high-quality film with the same wide bandgap shows significantly improved GB potential contrast and surface potential uniformity, indicating that the effect of surface defects is critical when examining GB charging using surface potential data. In addition, we discuss the effect of the SKPFM setup on the validity of potential measurement, to exclude possible artifacts due to improper SKPFM setups. The SKPFM results were corroborated by using SCM measurements on the films with a CdS buffer layer. The SCM image shows clear GB contrast, indicating different electrical impedance on the GB from the grain surface. Further, we found that the GB contrast disappeared when the CdS window layer was deposited after the CIGS film was exposed extensively to ambient, which was caused by the creation of CIGS surface defects by the ambient exposure.**

Index Terms — **CIGS, grain boundary, surface potential scanning Kelvin probe force microscopy, scanning capacitance microscopy.**

I. Introduction

The electronic and electrical properties of the grain boundaries (GBs) in polycrystalline $Cu(In,Ga)Se_2$ (CIGS) thin films have attracted great interest, as high-performance CIGS solar cells [1]–[3] have reached the record conversion efficiency of E_{ff}>20%, the highest among the thin-film solar cells; this is significantly higher than that achieved by its single-crystal counterpart [4]. A critical question arises: Are the GBs in this polycrystalline film active as non-radiation recombination centers (similar to most thin-film materials such as Si), benign or inactive for the recombination, or even beneficial for photovoltaic through three-dimensional minority carrier collection? A large number of microscopic characterization efforts have been taken to address this issue. Using scanning Kelvin probe force microscopy (SKPFM) [5,6] to map the surface electrostatic potential (or workfunction by reversing the potential contrast over the image) is a major effort that has resulted in a number of research articles [7]–[18]. Despite the fact that SKPFM measures the surface potential that relates to the surface defect/charge, and that the surface potential is screened out from the film bulk within a shallow depletion distance of ~50–300 nm from the surface, the articles attempt to interpret the data in terms of film bulk or to reflect the bulk property using the surface potential data. Nevertheless, the reported surface potential or workfunction images and the subsequently proposed GB charging are highly inconsistent across the articles [7]–[18]. Because SKPFM gives a surface potential contrast rather than absolute potential values, all kinds of GB potential contrast are reported: a peak at the GB corresponding to a positively charged GB, a potential dip to a negatively charged GB, a flat potential through the GB, and a potential step across the GB. The latter two cases correspond to neutral GBs, and the difference is whether or not the Fermi level (E_F) across the GB is aligned. Only potential peaks at the GBs were reported in some articles [7]–[9],[11]–[14], and all the different types of potentials were observed within one potential image in the other articles [10,17]. A conclusive understanding of this high inconsistency is desirable.

We have previously published SKPFM results measured on our high-performance films, which gave rise to consistently positively charged GBs [7]–[9]. In this paper we revisit the measurement with new experimental methods and data, and comment on the possible reasons for the inconsistency reported in this specific study. We suggest that, first of all, whether a measurement is valid or the data truly reflect the surface potential must be closely examined; second, what the potential contrast directly means must be clarified; and third, whether the measured GB potential contrast on the surface can be extrapolated to a certain depth deeper than the surface depletion width should be discussed. We start with the second issue, and address the first and the third with our experimental facts and results.

II. Effect of Surface Defects and Charges

To simplify the discussion of the effect of surface charge on the interpretation of GB potential contrast, we assume a uniform and defect-free subsurface region. As SKPFM measures the surface potential, the potential contrast reflects the charge density difference between the GB and the grain surface nearby. A potential peak on the GB can be interpreted for all three cases of a positively charged and a negatively charged GB, and the neutral GB (Fig. 1), i.e., how the GB is charged depends on the surface defects/charges around the

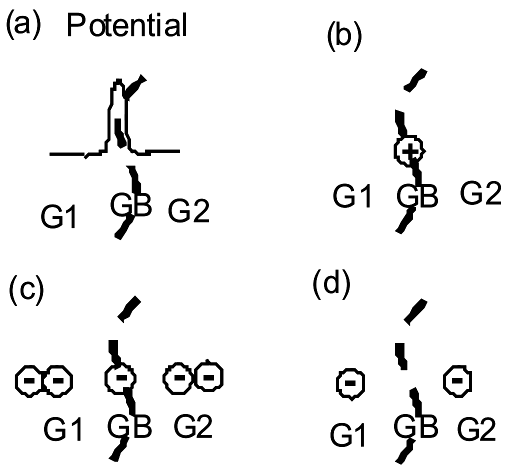

Fig. 1. A schematic illustrating that (a) a GB potential peak can be interpreted for all the cases of (b) a positively and (c) a negatively charged GB, and (d) a neutral GB, depending on the surface charges/defects around the GB.

GB. Therefore, having a well-controlled film surface that is defect free, or at least a uniformly charged surface, is a critical pre-condition for this specific effort. Nevertheless, the defect and charge configuration of this thin film, especially at the surface layer, is complicated and sensitive to the detailed fabrication processes. For example, several seconds of In-termination before ending the third stage of the three-stage co-evaporation, which is supposed to modify a few surface atomic layers of the film, is considered the main reason for improved device fill factor (FF) by improving defects of the surface layer [2]. Considering the small potential contrasts (~50–300 mV) reported in the literature [7]–[18], charges surrounding the GB with moderate fluctuations of the defect levels can readily confuse, blur, or even reverse the GB potential contrast.

To overcome this uncertainty, our approach is to measure on controlled high-performance films. These films are expected to have minimal surface defects due to the high-quality diode ideality factor after the films were made into devices [2,3]. This ideality factor indicates a minority-carrier-diffusion-dominated carrier transport that should happen only without dense interface states at the junction. Indeed, our SKPFM measurements show well-defined GB potential contrast only on the high-performance films. If the film quality is low (efficiency of devices made of the films is low), we can no longer observe clear potential contrast on the GB, which is consistent with the above discussion that the GB potential contrast depends strongly on the surface defects. In this light, the potential image quality including the potential uniformity over the grain surface and the GB contrast can be regarded as a qualitative reference of the material quality of the surface layer.

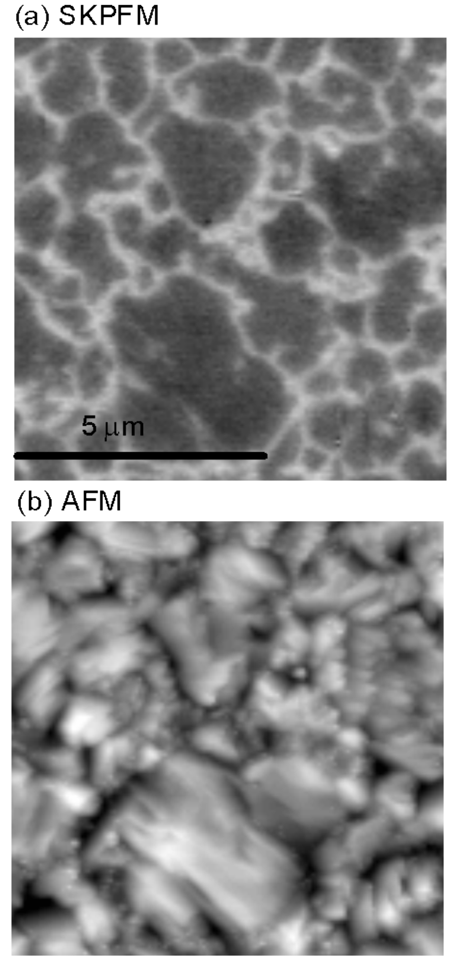

Fig. 2. (a) SKPFM and (b) the corresponding AFM images taken on a high-performance CIGS film with a Ga content of 30% and bandgap of 1.1 eV. Grey scales are 400 mV in the potential image and 200 nm in the AFM image.

In a previous publication [8], we reported that the GB potential contrast dropped sharply with increasing Ga content, Ga/(In+Ga), or bandgap. Our typical high-performance film has a 28%–30% Ga content and ~1.1 eV bandgap; the potential and AFM images are shown in Figs. 2(a) and 2(b). Slightly increasing the Ga content to 40% and bandgap to 1.2 eV caused significant device degradation. Correspondingly, we have observed significant degradations of the GB potential contrast and the potential uniformity across the grain surface [Figs. 3(a) and 3(b)]. The CIGS group at the National Renewable Energy Laboratory (NREL) has recently reported a significant improvement in the high bandgap devices and has shown that the open-circuit voltage (V_{OC}) improvement is due to the improvement of dark saturation current and diode ideality factor [19]. This clearly indicates an improvement of the junction defects, which relate to the film surface defects before the window layer was deposited or the junction was

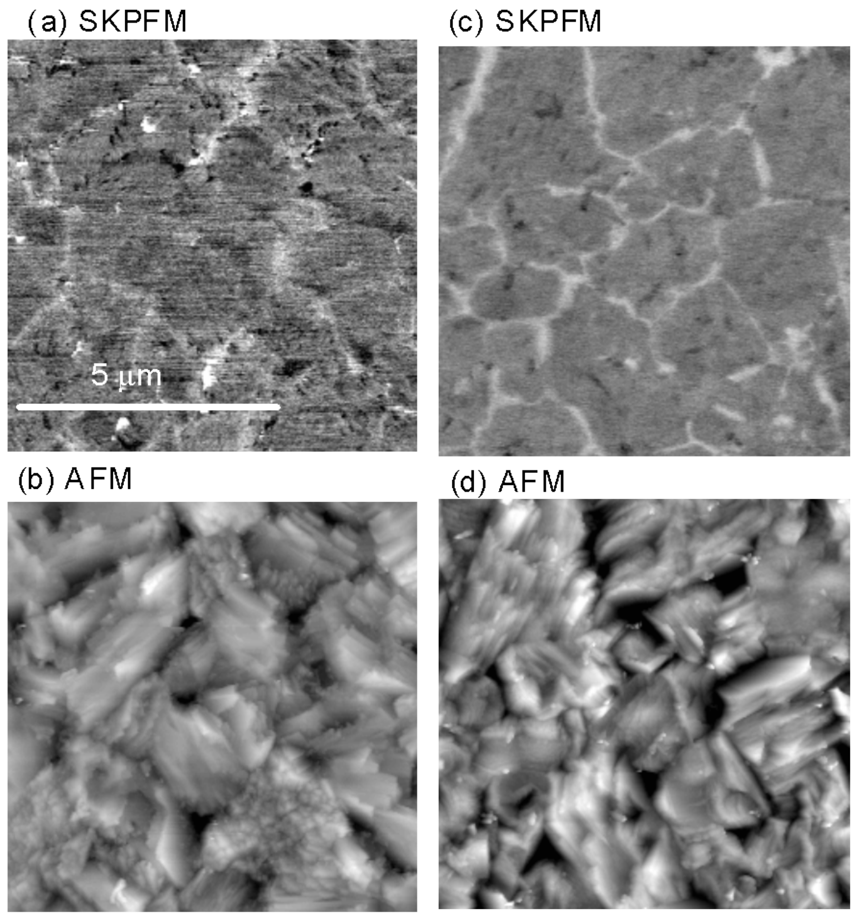

Fig. 3. (a) (c) SKPFM and (b) (d) the corresponding AFM images taken on (a) (b) low-performance and (c) (d) high-performance CIGS films with a wide bandgap of 1.2 eV. Grey scales are 400 mV in the potential images and 200 nm in the AFM images.

formed. Our potential image also shows corresponding improvement of the potential uniformity and the GB potential contrast on this improved high bandgap film [Figs. 3(c) and 3(d)], indicating the importance of the grain surface defects when understanding and interpreting the GB potential contrast. The GB potential contrast drop in the low-performance, high-bandgap films can be due to the surface defects and/or a reduced GB potential. Therefore, it is conclusive that, without a high surface material quality, the GB charging cannot be determined solely by the GB potential measurement, which has been the main subject in the literature but has not been adequately addressed [7]–[18]. It is worth noting that the potential measurement is associated with two crucial aspects of the device performance: the grain surface defects with the junction quality and the GB potential with the GB recombination activity.

III. Critical Setup of Scanning Probe Force Microscopy

We discuss the critical effects of the measurement setup on potential measurements. During the SKPFM measurement, we found that the potential images are highly sensitive to the details of the experimental setup. Especially in the current interest of a small GB potential contrast (down to <50 mV in the literature [10,13]), the potential contrast could even be reversed by different setups, resulting in reversed GB charging. Therefore, the data/image quality and consistency is critical here, as it affects the result not only in quantitative magnitude but also potentially in a qualitative way or by making the result inconclusive.

Our setup uses the amplitude-modulation mode for AFM and the low-frequency (~20 KHz) amplitude mode for SKPFM. Our AFM and SKPFM are in both ambient (Thermomicroscope CP) and Argon glove box (Veeco D5000 with Nanoscope V controller, H_2O, and O_2 <0.1 ppm), which both give consistent results and thus exclude the possibility of a water layer on the surface, which is questioned in the

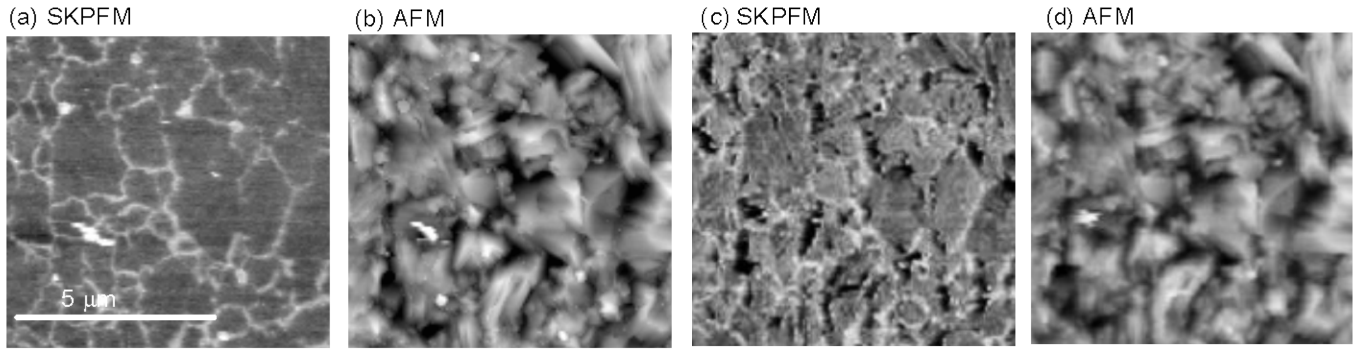

Fig. 4. (a) (c) SKPFM and (b) (d) the corresponding AFM images taken on the same area of a high-performance, 1.1-eV-bandgap film using (a) (b) the low frequency and (c) (d) the second harmonic frequency SKPFM setups. Grey scales are 400 mV in the potential images and 200 nm in the AFM images.

community. The AFM image quality is a critical factor for the validation of the potential image with this small amount of contrast. The tip was brought to a proximal distance (10 nm) when the potential image was taken in order to enhance the spatial resolution. The potential measurement is more sensitive to small deviations from the AFM constant settings than the corresponding AFM image. Closely examining the AFM image quality is necessary to determine the validity of a potential measurement. If noise level in the AFM image is high, or features of crystal facets (as shown in Figs. 1 and 2) are not clearly visible, the validity of the more sensitive potential scan is highly doubted. To achieve high-quality AFM imaging on the CIGS films with ~200-nm rough corrugations, adequately fast feedback control is necessary, and it cannot be fully compensated by a slow scan. Therefore, we used the amplitude-modulation AFM as our primary system for this specific case of CIGS film with rough corrugations, after examining and comparing the details of a setup with an ultra-high vacuum (UHV) AFM (Omicron VT-AFM) that has to use the frequency-modulation mode with an intrinsic slow feedback due to the very narrow cantilever resonance width (10 Hz order) in UHV.

Our SKPFM setup is capable of using either a low frequency (~20 KHz) or the second harmonic frequency (250–400 KHz); the latter gives a higher potential sensitivity due to the resonance of the cantilever oscillation [6]. However, we found that the image quality using the resonant frequency mode is affected by a significantly heavier topographic effect than the low-frequency mode. In potential measurement on a flat surface (<20-nm corrugations in similar lateral feature sizes of ~μm) such as an epitaxial material, we used the resonant frequency mode, and the topographic effect was negligible. However, for measurements on the rough thin-film surfaces, especially when targeting at the small potential contrast, the topographic effect can be misleading and catastrophic. Figures 4(a) and 4(c) show SKPFM images taken on the same area of the high-efficiency CIGS sample. The data of Fig. 4(a) was taken using the low-frequency mode, while that of Fig. 4(c) was taken using the second harmonic frequency. It is evident that significantly different conclusions might be drawn from one sample based on variations induced by measurement conditions.

IV. Scanning Capacitance Microscopy Imaging

We further carried out scanning capacitance microscopy (SCM) [22] measurement, another AFM-based nm-resolution electrical imaging technique. The SCM data can be used to corroborate features observed in SKPFM by taking SCM and SKPFM on the same surface area (Fig. 5). The SCM measurement (Veeco D3100 and D5000 with Nanoscope V in both ambient and Ar glove box) involves a junction, the capacitance of which is targeted. In the well-established SCM characterizations on Si [22], the junction is at the metal-insulator-semiconductor (MIS) structure, and only the capacitance is measured due to adequately high resistance through the high-quality and very thin (a few nm) SiO_x layer. However, the MIS structure on the CIGS thin film with a high quality (defect-free in the layer and at the interface) and a few-nm-thin insulator layer is currently not reached. We instead deposited a CdS window layer by chemical bath deposition (CBD), which is used to make our high-performance devices [2,3]. However, unlike the MIS structure, this structure contains a significant electrical conduction, which makes the interpretation of the measurement complicated. Although the SCM image [Fig. 5(c)] shows clear contrast on the GBs, we cannot conclude a reversed polarity of the GB, because the overall signal level shifts and changes its sign with applying a tip-sample DC bias due to the significant contribution of the electrical conduction. However, the clear and uniform SCM contrast on the GBs indicates that the GB electrical property is different from the grain surface. The consistent SCM and SKPFM results on the GBs, as recognized from the images taken in the same surface area [Figs. 5(c) and 5(a)], indicate that the SCM and SKPFM contrasts have the same physical origin.

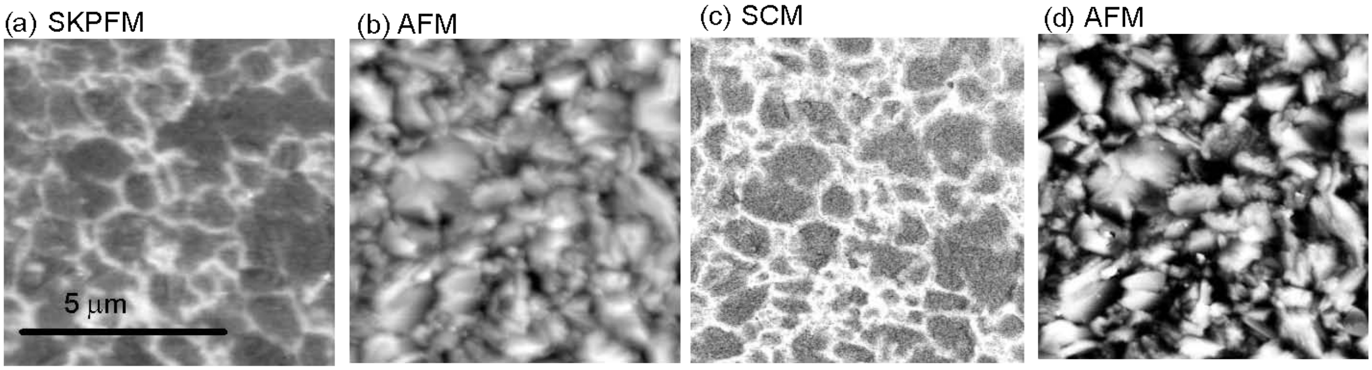

Fig. 5. (a) SKPFM and (c) SCM images taken on the same sample area of a high-performance CIGS film with a bandgap of 1.1 eV. (b) and (d) are the corresponding AFM images to (a) and (c). Grey scales in the SKPFM, SCM, and AFM images are 400 mV, 2 V, and 200 nm, respectively.

The SCM contrast changed significantly when the CIGS film was exposed to ambient before the CdS window layer was deposited (Fig. 6). If the exposure time is short, e.g., 12 minutes [Fig. 6(a)], the GB contrast is still clear, similar to the case without the exposure [Fig. 5(c)]. However, if the exposure time is long, e.g., 24 hours [Fig. 4(c)], the SCM contrast disappears. Of course, this ambient exposure cannot cause a significant change in the GB structure so that the GB electrical property is the same as the grain surface. However, the exposure can create significant defects in the surface and near-surface regions of the film [23]. After the CdS window layer is deposited on the film, the junction property should be dominated by the significant defects at the CdS/CIGS interface. The defects created during the ambient exposure should cover both the grain surface and the GBs, which makes no difference between the grain surface and GB, causing the GB contrast to disappear.

The combination of SCM and SKPFM contrasts with high device performance is most consistent with GB inversion, rather than depletion. Whether the GB is depleted or inversed cannot be determined solely by the potential measurement, as previously discussed [7]. However, if the GB is depleted, there are likely deep levels that would make it difficult to reach the current high device performance. If it is inverted, there are not necessarily deep levels; shallow donors can be responsible, and the donor states are not recombination centers. Na in CIGS films deposited on soda lime glass substrate has been extensively discussed [24,25] and unambiguously probed by atom probe tomography (APT) [26]–[28]. Interstitial Na at the GBs is a shallow donor [9]. The Na content is as high as 1 at% at the GBs [26,27], which is more than adequate to pin the E_F at the shallow donor levels [9]. If the inverted GB extends into the film bulk by a certain distance over the junction depth, it could facilitate the three-dimensional minority carrier collection and benefit the device performance [29,30]. Another hypothesis about the effect of GB inversion is that it could improve the junction quality at the GB, compared with the junction at the grain surface, after the junction is fully formed as the device is completed.

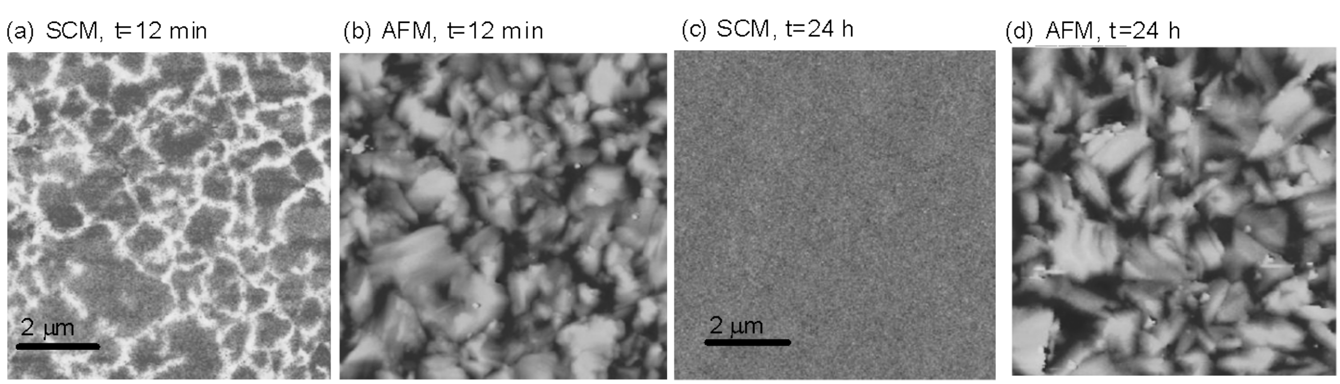

Fig. 6. (a) (c) SCM and (b) (d) the corresponding AFM images taken on the CdS/CIGS structures where the CIGS was exposed to ambient for (a) (b) 12 minutes and (c) (d) 24 hours before the CdS layer was deposited. The grey scales are 3 V and 200 nm in the SCM and AFM images.

V. Summary

We revisited the issue of CIGS surface potential and GB charging by performing SKPFM measurements on both high- and low-quality wide-bandgap films and by using complementary SCM measurements. The differences in grain-surface potential uniformity and GB potential contrast between the high- and low-quality films are due to surface defects and charges, demonstrating that a high material quality of the film surface is a necessary precondition for determining GB charging by SKPFM surface potential measurements. A high-quality potential image with a uniform grain surface potential and clear GB potential contrast indicates both a high-quality film surface with minimal surface defects/charges and inverted/depleted GBs. The SKPFM results show consistent positively charged GBs in our high-quality CIGS films. The SCM result shows consistent GB contrast and demonstrates the different impedance on the GBs from the grain surface. Our experiments further show that the potential measurement results depend closely on the SKPFM setup. We discussed the effects of GB charging on GB recombination activity and photovoltaic device performance.

Acknowledgements

This work was supported by the U.S. Department of Energy under Contract No. DOE-AC36-08GO28308 with the National Renewable Energy Laboratory.

References

[1] P. Jackson, D. Hariskos, E. Lotter, S. Paetel, R. Wuerz, R. Menner, W. Wischmann, and M. Powalla, Prog. Photovolt: Res. Appl. 19, 894 (2011).
[2] I. Repins, M.A. Contreras, B. Eggas, C. DeHart, J. Scharf, C.L. Perkins, B. To, and R. Noufi, Prog. Photovolt: Res. Appl. 16, 235 (2008).
[3] M.A. Contreras, K. Ramanathan, J. AbuShama, F. Hasoon, D.L. Young, B. Egaas, and R. Noufi, Prog. Photovolt: Res. Appl. 13, 209 (2005).
[4] C. H. Champness, Proceedings of the 29th IEEE PVSC Conference (IEEE, Piscataway, 2002), p. 732; L. S. Yip and I. Shih, Proceedings of the First World Conference on Photovoltaic Energy Conversion (IEEE, Piscataway, 1994), p. 210.
[5] M. Nonnenmacher, M.P. O'Boyle, and H.K. Wickramasinghe, Appl. Phys. Lett. 58, 2921 (1991).
[6] A. Kikuhara, S. Hosaka, and R. Imura, Appl. Phys. Lett. 66, 3510 (1995).
[7] C.-S. Jiang, R. Noufi, J.A. AbuShama, K. Ramanathan, H.R. Moutinho, J. Pankow, and M.M. Al-Jassim, Appl. Phys. Lett. 84, 3477 (2004).
[8] C.-S. Jiang, R. Noufi, K. Ramanathan, J.A. AbuShama, H.R. Moutinho, and M.M. Al-Jassim, Appl. Phys. Lett. 85, 2625 (2004).
[9] Y. Yan, C.-S. Jiang, R. Noufi, S.H. Wei, H.R. Moutinho, and M.M. Al-Jassim, Phys. Rev. Lett. 99, 235504 (2007).
[10] R. Baier, D. Abou-Ras, T. Rissom, M.C. Lus-Steiner, and S. Sadewasser, Appl. Phys. Lett. 99, 172102 (2011).
[11] M. Takihara, T. Minemoto, Y. Wakisaka, and T. Takahashi, Proceedings of the 35th IEEE PVSC Conference (IEEE, Piscataway, 2010), p. 002512.
[12] M. Takihara, T. Minemoto, Y. Wakisaka, and T. Takahashi, Prog. Photovolt: Res. Appl., in press.
[13] D.F. Marron, S. Sadewasser, A. Meeder, T. Glatzel, and M.C. Lux-Steiner, Phys. Rev. B 71, 033306 (2005).
[14] S. Sadewasser, Thin Solid Films 515, 6136 (2007).
[15] S. Siebentritt, S. Sadewasser, M. Wimmer, C. Leendertz, T. Eisenbarth, and M.C. Lux-Steiner, Phys. Rev. Lett. 97, 146601 (2006).
[16] S. Siebentritt, T. Eisenbarth, M. Wimmer, C. Leendertz, F. Streicher, S. Sadewasser, and M.C. Lux-Steiner, Solid Thin Films 515, 6168 (2007).
[17] Z. Zhang, X. Tang, U. Lemmer, O. Kiowski, M. Powalla, and H. Holscher, Proceedings of the 37th IEEE PVSC Conference (IEEE, Piscataway, 2011), p. 134, in press.
[18] A.R. Jeong, R.H. Shin, W. Jo, J. Gwak, S. Ahn, J.H. Yun, and K. Yoon, Proceedings of the 37th IEEE PVSC Conference (IEEE, Piscataway, 2011), p. 116, in press.
[19] M.A. Contreras L.M. Mansfield, B. Egaas, J. Li, M.R. Romero, R. Noufi, W. Rudiger-Voigt, and W. Mannstadt, Proceedings of the 37th IEEE PVSC Conference (IEEE, Piscataway, 2011), p. 18, in press.
[20] S. Ono, M. Takeushi, T. Noda, and T. Takahashi, Jpn. J. Appl. Phys. 42, 4869 (2003).
[21] Y. Rosenwaks, R. Shikler, T. Glatzel, and S. Sadewasser, Phys. Rev. B 70, 085320 (2004).
[22] For a review, see C.C. Williams, Annu Rev. Mater. Sci. 29, 471 (1999).
[23] W.K. Metzger, I. L. Repins, and M.A. Contreras, J. Appl. Phys. 93, 022110 (2008).
[24] S.-H. Wei, S.B. Zhang, and A. Zunger, J. Appl. Phys. 85, 7214 (1999).
[25] A. Rockett, Thin Solid Films 480, 2 (2005).
[26] F. Couzinie-Devy, E. Cadel, N. Barreau, L. Arzel, and P. Pareige, Appl. Phys. Lett. 99, 232108 (2011).
[27] F. Couzinie-Devy, E. Cadel, N. Barreau, P. Pareige, and J. Kessler, Proceedings of the 37th IEEE PVSC Conference (IEEE, Piscataway, 2011), p. 571, in press.
[28] O. Cojocaru-Miredin, P.-P Choi, D. Abou-Ras, S.S. Schmidt, R. Caballero, and D. Raabe, Proceedings of the 37th IEEE PVSC Conference (IEEE, Piscataway, 2011), p. 570, in press.
[29] E. Christoffel, M. Rusu, A. Zerga, S. Bourdais, S. Noel, and A. Slaoui, Thin Solid Films 403, 258 (2002).
[30] G. Beaucarne, S. Bourdais, A. Slaoui, J. Poortmans, Proceedings of the 28th IEEE PVSC Conference (IEEE, Piscataway, 2000), p. 128.